PAPER

Check for updates

Electrochemical detection of fluoride ions in water with nanoporous gold modified by a boronic acid terminated self-assembled monolayer

Lara Marie Novak [ID] * and Eva-Maria Steyskal [ID]

Nanoporous gold (npAu) is a perfectly suited platform for the electrochemical detection of minor amounts of chemical species in solution due to its high surface-to-volume ratio. By surface-modification of the self-standing structure with a self-assembled monolayer (SAM) of 4-mercaptophenylboronic acid (MPBA) it was possible to create an electrode very sensitive towards fluoride ions in water, also suitable for mobile use in future sensing applications. The proposed detection strategy is based on the change in the charge state of the boronic acid functional groups of the monolayer, induced by fluoride binding. The surface potential of the modified npAu sample reacts fast and sensitively to stepwise F^- addition, showing highly reproducible, well-defined potential steps with a detection limit of 0.2 mM. Deeper insight into the reaction of fluoride binding on the MPBA modified surface was gained by electrochemical impedance spectroscopy. The proposed fluoride sensitive electrode exhibits a favorable regenerability in alkaline media, which is of central importance for future applications considering environmental as well as economical aspects.

1 Introduction

Detection of electroinactive anions, particularly in aqueous media, has been a topic of intensive research recently.[1,2] Especially halide anions have attracted attention due to their importance in biological systems. Fluoride, for example, is not only a very important trace element in the human body, but also can cause great harm to human health as well as the environment in larger doses.[3–5]

There are many different approaches for the detection of fluoride ions in water already. However, they often suffer from disadvantages such as costly and sophisticated instrumentation and no comprehensive solution to the problem has been found yet. For example, ^{19}F NMR, as well as many optical systems, are very precise tools for laboratory scale tests of water probes, but the apparatus is just not suitable for the in field operation, *e.g.* for *in situ* wastewater analysis.[5,6] Besides ion-selective electrodes, which often exhibit long detection times,[7] different other electrochemical electrodes have been proposed for the recognition of fluoride ions. Electrochemical sensing methods have gained a lot of attention, owing to their sensitivity, quick response, easy handling and low cost.[8–10] Some electrochemical approaches use redox active markers to produce a signal,[8,11] making an environmentally friendly use difficult due to water pollution. Recently, colorimetric or fluorescent approaches have been very popular since they are cost effective and simple, but still they often suffer from poor selectivity and accuracy or the

change in colour is simply irreversible.[12] Also, different novel and promising modifications of various surfaces have been studied, but often electroactivity is lost after few measurements caused by degradation or structural changes due to the attack of fluoride anions[13–15] or the preparation of those surfaces requires complex multistep procedures. This lack of simplicity in sensor preparation as well as in operation generally tends to be a problem in more sophisticated systems.[5,16,17] So till date, there is no universal technique for fluoride detection in water and still alternatives are looked for.

Over the past two decades, nanoporous gold (npAu) prepared by the method of electrochemical dealloying has become a very popular material in many sensing applications due to its good conductivity, high surface-to-volume ratio, free-standing structure and easy tunability.[18–20] However, as gold itself is not very sensitive to F^- and furthermore reacts stronger with other halogens such as chlorine ions,[21–23] a modification of its surface, *e.g.*, by the formation of self-assembled monolayers (SAMs) is needed to make it suitable for fluoride detection. The assembly of SAMs on (nanoporous) gold surfaces *via* thiol terminated molecules is well understood[19,24] and enables the development of fast responding sensors tailored towards specific chemical applications by choice of a suitable functional end group.

As possible candidates, boronic acid derivatives are widely known as fluoride receptors as they form complexes with hard bases such as fluoride anions due to their weak Lewis acidity. Upon F^- binding the boron center changes its hybridization from sp^2 to sp^3 which also leads to a change in geometry and charge state of the functional group.[25] As F^- anions are smaller and also stronger Lewis bases than other anions, they can be

Institute of Material Physics, Graz University of Technology, NAWI Graz, Petersgasse 16, 8010 Graz, Austria. E-mail: novak@tugraz.at

bound very specifically at the boron center, making boronic acid derivatives very selective to the analyte of discussion. Furthermore, F^{−} binding is favored at neutral pH values enabling application in water.[5,25] The concurring interaction of hydroxyl ions at alkaline pH values can be used to restore the functional group and therefor achieve reversibility.[5,11,16]

In this work we combined the various useful intrinsic characteristics of nanoporous gold with the unique fluoride sensitivity of boronic acid by surface modification of npAu with a 4-mercaptophenylboronic acid (MPBA) SAM. The here presented sensing strategy profits from the change in charge of the boronic acid moiety upon fluoride binding, which results also in a change of the surface potential of the modified npAu sample. Thus, an easily measurable electrochemical signal is produced, without the need of additional redox markers. The nanoporous sensor can be easily fabricated and shows a good sensitivity (down to 0.2 mM) towards fluoride ions in water. The presented system is simple and compact, making it suitable for real-time *in situ* studies, which is of utmost importance for many envisioned future applications, *e.g.* thinking of mobile devices for environmental sensing.[26] Moreover, the exploited binding mechanism is easily reversible by alkaline treatment, making the electrode re-useable many times without a loss of detection quality.

2 Experimental procedures

2.1 Chemicals

4-Mercaptophenylboronic acid ($HSC_6H_4B(OH)_2$, MPBA, 90%), 0.1 M sodium fluoride aqueous solution (NaF, analytical standard for ion-selective electrodes) and 1 M perchloric acid ($HClO_4$, >99%) were purchased from Sigma Aldrich. Potassium hydroxide (KOH, ≥85%), potassium nitrate (KNO_3, ≥ 99%) and sodium chloride (NaCl, ≥99.5%) were purchased from Carl Roth. Mentioned chemicals, except MPBA, were diluted or dissolved in high purity water (ROTIPURAN, Carl Roth) to the desired concentration. MPBA was dissolved in ethanol (Carl Roth).

2.2 Sample preparation and characterization

Electrochemical preparation and sensing experiments were performed in a three electrode setup using a commercial Ag/AgCl (3 M KCl with 3 M KNO_3 salt bridge) electrode as the reference, in relation to which all potentials hereafter are given.

The nanoporous gold electrodes were prepared from an Au–Ag (25 at%/75 at%) master alloy by a potential controlled dealloying process similar to previous work of our group.[19] Summing up briefly, dealloying was performed in 0.1 M $HClO_4$ with a Pt-wire counter electrode under chronoamperometric conditions at $U_{Ag/AgCl} = 1100$ mV until the current had fallen below 50 μA. Subsequently, after careful rinsing, electrochemical reduction of the primary oxide *via* cyclic voltammetry was done with a scan rate of 0.5 mV s^{−1} between −200 and 1200 mV for two cycles in 0.1 M $HClO_4$, followed by 40 cycles in 1 M KOH between −1000 and 600 mV with a scan rate of 2 mV s^{−1} to achieve a steady state for the following studies. To determine the active surface area (approximately 11 m[2] g^{−1}) and pore size (15–20 nm) of the dealloyed samples, the method described by Lakshmanan *et al.*[27] was followed, using the scan rate dependence of the current in the double layer regime, assuming a specific double layer capacity of 40 μF cm^{−2} in $HClO_4$.[27] For the sensing experiments, self-assembling monolayers were deposited by immersing the npAu samples in an 8 mM solution of MPBA in ethanol for 72 h followed by drying for 30 minutes and soaking in ultra pure water (1 h) and 1 M KOH (1 h). The regeneration of used sensor electrodes was done by soaking them in 1 M KOH overnight.

2.3 Electrochemical sensing techniques

The sensing measurements were performed using a Metrohm potentiostat and controlled *via* the accompanying NOVA 1.11 software.

Sensing based on changes of the surface potential was performed in open circuit potential (OCP) mode using an Autolab PGSTAT204 potentiostat. A coiled gold wire was used as counter electrode. OCP measurements were performed in a cell containing 10 ml of high purity water. Addition of the halogen ions was done during the running measurements by adding the desired volume of NaF or NaCl solution stepwise, resulting in maximum final concentrations of 4 mM.

Since for electrochemical impedance spectroscopy (EIS) a conductive solution is required from the beginning, 20 ml of 50 mM KNO_3 aqueous solution was used as background electrolyte. Samples were measured in this electrolyte without, directly after and one day after the addition of 4 mM NaF. For EIS an Autolab PGSTAT128N potentiostat with an electrochemical impedance spectroscopy module (FRA32M) was used. A coiled Pt-wire served as counter electrode and a parallel capacitance of 1 mF was connected to the reference to reduce its impedance at high frequencies. Frequency spectra were recorded at open circuit potential with frequencies in a range from 10 mHz to 100 kHz using an amplitude with a round mean square (RMS) value of 20 mA.

Before starting each anion sensing measurement, samples were soaked in the starting electrolyte for at least 8 h to ensure diffusion into the porous structure. All data presented in this study result from a well balanced, regenerated sensor. To regenerate the samples they were soaked in 1 M KOH overnight after each fluoride detection measurement.

3 Results

In the present work, npAu is surface-modified with self-assembled monolayers of MPBA (molecular structure see inset Fig. 1) for the detection of F^{−}, as gold itself is not very sensitive to fluoride. For the purpose of the successful assembly of the monolayer, binding was verified by electrochemical impedance spectroscopy. After SAM modification the Bode plot (Fig. 1) has an increased impedance compared to pristine npAu as easily visible in the Bode modulus plot, confirming the presence of an insulating layer on the electrode's surface.[28] Furthermore, the phase angle moves towards −90° in the low frequency regime as
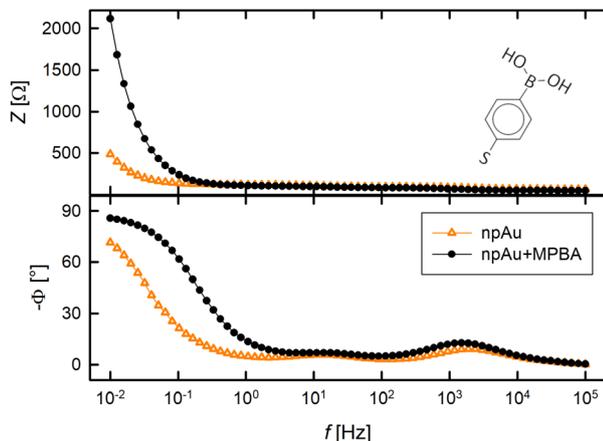
Fig. 1 Bode plot of the npAu electrode with (black) and without (orange) a layer of MPBA. Inset on the upper right shows the molecular structure of 4-mercaptophenyl boronic acid (MPBA).

shown in the Bode phase plot in Fig. 1, indicating a smoother surface due to the formation of the SAM.[28] Additionally, the binding process of MPBA on the gold surface was monitored by *in situ* resistometry as a highly sensitive diagnosis tool for ad- and desorption processes, well established in our group.[19] Compared to the bare nanoporous electrode, the resistance finally increased 6% upon MPBA assembly (measurement not shown).

With the modified working electrode, a strong response of the surface potential can be detected upon fluoride addition *via* OCP measurements as can be seen in Fig. 2a. Starting with the sample immersed in high purity water, NaF was added to the measurement cell, stepwise increasing the concentration of the analyte as indicated by the blue arrows. Immediately after fluoride is added, a strong response of the electrode is visible, settling to a new equilibrium potential after a short time. The change in the open circuit potential is strongest for the first addition step, afterwards the potential change upon F^- addition decreases exponentially.

Due to the high sensitivity of the modified sample, small concentrations of fluoride ions are already observable.

Precisely, fluoride addition in steps as low as 0.2 mM (Fig. 2b) could be successfully detected, leading to a correspondingly smaller, but still well-defined response in the measured potential. A common trend of the potential changes in both independent addition rows becomes evident in Fig. 2c, where the mean value of each ΔU_{OCP} step is plotted over the NaF concentration for the addition rows from (a) (black circles) and (b) (gray dots). These two cases can be described by a common exponential decay function as discussed in detail below. In particular, the good agreement of rows (a) and (b) becomes evident at a F^- concentration of 1 mM, which is covered in both addition series.

Further insights to the F^- sensitivity are provided by EIS. Fig. 3 shows the resulting frequency spectra of the MPBA modified npAu electrode before (red), directly after (black) and one day after (blue) the addition of fluoride. As in the case of EIS a conductive electrolyte is needed, measurements were performed in 50 mM KNO_3. By choosing the concentration of the background electrolyte rather high in comparison to that of the added NaF (4 mM), the impact of the change in conductivity on the recorded data was kept small, enabling a better comparison between the measurements with and without fluoride. Data are presented in form of a Nyquist plot showing three specific frequency regimes, starting from high frequencies on the left to low ones on the right (Fig. 3a). Subplots (b) and (c) provide details of the high and low-to-mid-frequency regime, respectively.

A semicircle appears in the high frequency regime of all measurements caused by the gold wire used to contact the sample. In the mid-frequency regime of the measurement without fluoride (red curve) a quarter circle manifests, followed by a steep increase of the imaginary part of the impedance at low frequencies. Especially in Fig. 3b it is immediately apparent that the slope of the increasing imaginary part of the impedance in the low frequency regime becomes steeper after fluoride addition (black and blue curve). This means that there is a slight shift of the phase angle more towards −90°, indicating that the purely capacitive part of the response is a little higher with the analyte present. In subplot (c), the second semicircle in the mid-frequency regime is clearly less pronounced for the measurement right after fluoride addition (black) than without. One day
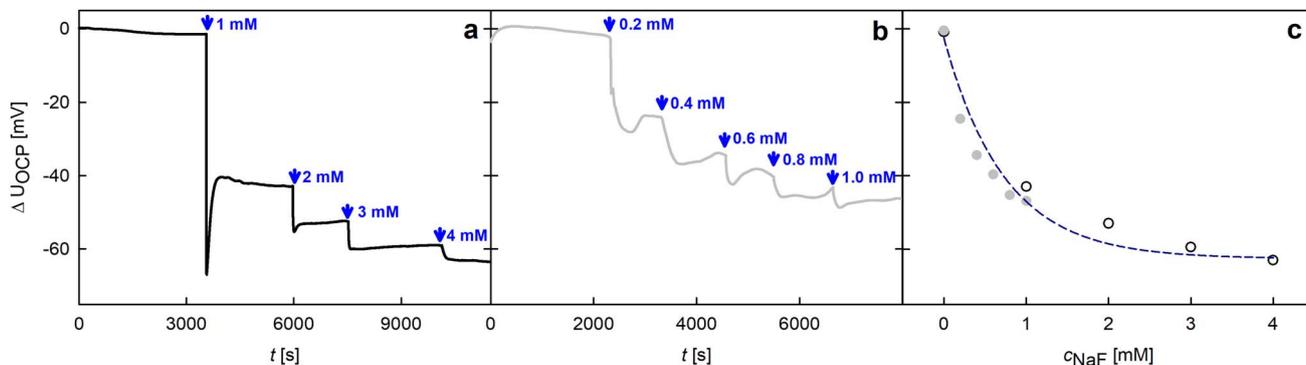

Fig. 2 Change of the open circuit potential (ΔU_{OCP}) of a MPBA modified npAu electrode over time t upon different F^- concentration changes (c_{NaF}). (a) 1 mM steps, (b) 0.2 mM steps, (c) shows a direct comparison of the mean ΔU_{OCP} changes of (a) and (b) as a function of concentration.
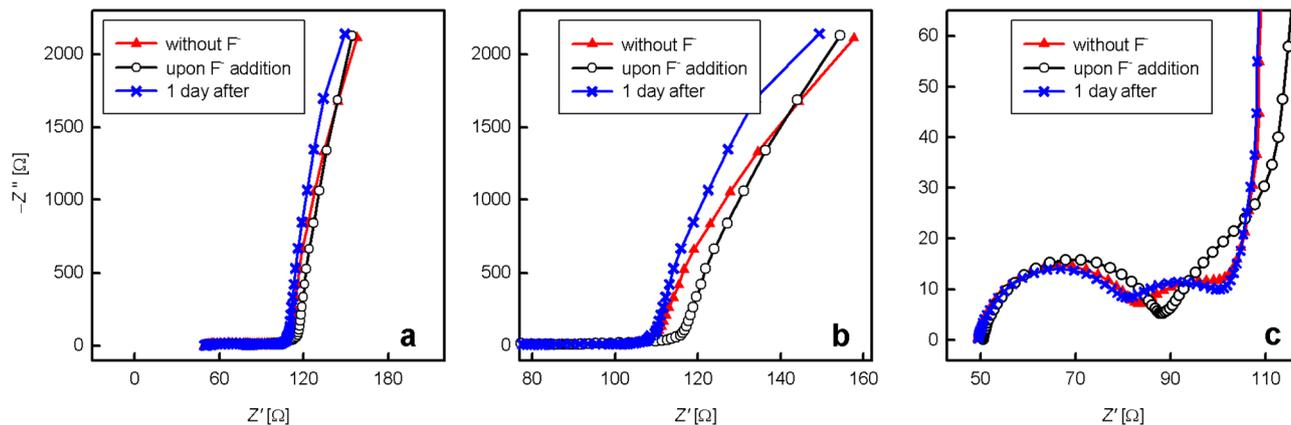
Fig. 3 Nyquist plot of a MPBA modified npAu electrode in KNO_3 (red) upon fluoride addition (black) and after one day waiting time in 4 mM NaF (red). The whole plot is shown in (a), (b) shows a zoom of the low- and (c) of the high-to-mid-frequency regime. Note, that for the sake of better visibility of the discussed features, the Z' and $-Z''$ axis in (a) and (b) do not present similar intervals.

after addition (blue), the curve has the initial circle-like shape again. This behaviour immediately after the addition of the analyte can be assigned to ongoing charge transfer taking place, which again shows the adsorption of the fluoride anions and the resulting change in the surface state of the np electrode.[28–30]

One possible weakness emerging for fluoride sensors is their insufficient selectivity caused by the co-sensing of other halogen ions, especially Cl^-, due to the chemical affinity of the ionic species. Gold is particularly affected as it strongly reacts with chlorine and has a rather weak interaction with fluoride ions.[21–23] By modifying the gold surface with a monolayer of

MPBA, a remedy was found as presented in Fig. 4, which will be discussed in the following. To start with, the fluoride sensitivity due to the chosen surface modification is compared to that of bare npAu by means of ΔU_{OCP}. Fig. 4c schematically shows the reaction of the fluoride anions with the functional groups of the MPBA layer immobilized on the gold surface. Previous work of our group[19] demonstrates that the surface coverage of the SAM is smaller than one monolayer. Still, the fluoride anions exclusively interact with the boronic acid functional unit of the SAM and not with the gold surface, which becomes visible when comparing the change in surface potential for a pristine and
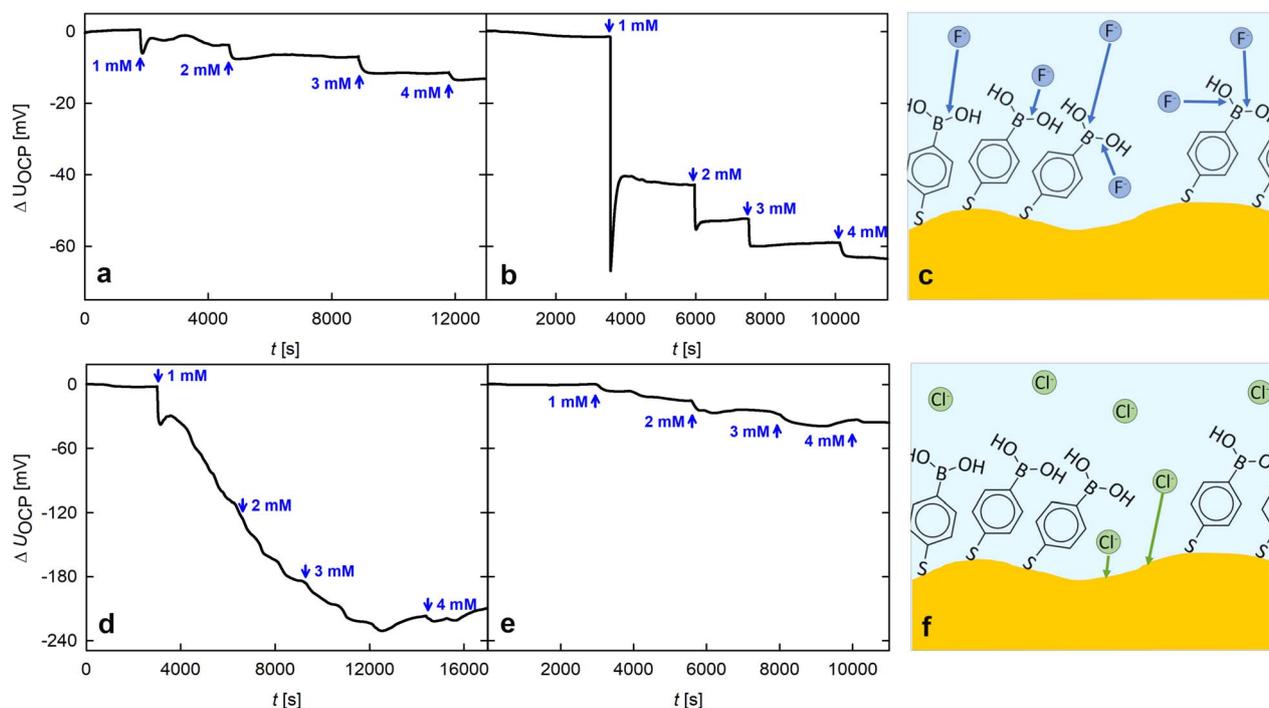

Fig. 4 ΔU_{OCP} of a bare (a and d) and a MPBA modified (b and e) npAu electrode upon 1 mM NaF (a and b) and 1 mM NaCl (d and e) addition. (c) and (f) show the schematic binding of the corresponding anions F^- and Cl^- at the MPBA-npAu system.

a MPBA-modified npAu platelet evinced in subplots (a) and (b), respectively. At the beginning of the measurement the electrolyte was high purity water and NaF was added in 1 mM steps as described before. Both data sets were adjusted to the same voltage scale, clearly visualizing the highly increased response to fluoride ions by the MPBA functionalization.

Besides the improved sensitivity to F$^-$, a positive side effect is the decreased response of the modified electrode to NaCl. In subplot (f), a scheme of the interaction of the sample with the ionic species is illustrated. As indicated by literature,[22,23] pristine gold strongly interacts with chloride ions. The corresponding measurement of an unmodified npAu sample's potential (Fig. 4d) shows a strong response of undefined behavior with a strong drift towards more negative values upon the addition of chloride. When a MPBA layer is present (Fig. 4e), this effect is weakened dramatically. As the MPBA layer itself is not very sensitive to Cl$^-$,[5] this signal decrease is assigned to the SAM acting as a protective layer, leading to a limited access for the chloride ions to the gold surface. The remaining signal presumably results from defects in the SAM where the Cl$^-$ ions still can react with the gold surface, as illustrated in scheme (f). When comparing the response of the modified sample (Fig. 4b and e) to the different halogen species, the ΔU_{OCP} steps are much less defined when Cl$^-$ is added. Also the potential change is smaller compared to the equivalent experiment using F$^-$, which underlines a good selectivity towards fluoride.

As displayed in Fig. 2 and 4, the intensity of the potential response upon fluoride addition decreases with each addition step due to increasing occupation of the boronic acid moieties. However, it is known from literature[5,25] that the hybridization of the boron center can be reversed upon ion-exchange reactions of F$^-$ to OH$^-$ in alkaline conditions, thereby enabling the reuse of the electrode without renewing the SAM, which is an important criterion for sustainable electrodes.[31] The regeneration capability was successfully checked for by successive potential measurements with a freshly prepared and (several times) KOH regenerated sample (see experimental section for details). For reasons of good comparability, all potential measurements presented in this study result from one and the same sample. Still, those addition rows were performed several times with different MPBA modified npAu samples, always resulting in a similar, well defined behaviour, freshly prepared as well as after KOH regeneration (data not shown). This emphasizes the good reproducibility of the response upon fluoride addition, which is crucial for future applications. A plot comparing the measurement data generated with an exemplary freshly prepared and KOH regenerated sample can be seen in Fig. 5. Upon fitting the data as an exponential function as given by the dashed line in Fig. 5 it is clearly visible that the mean potentials of both measurement series follow the same exponential trend.

4 Discussion

The central result of the presented study is that nanoporous gold, modified with a self assembled monolayer of MPBA, is highly sensitive to fluoride ions and well suitable for their
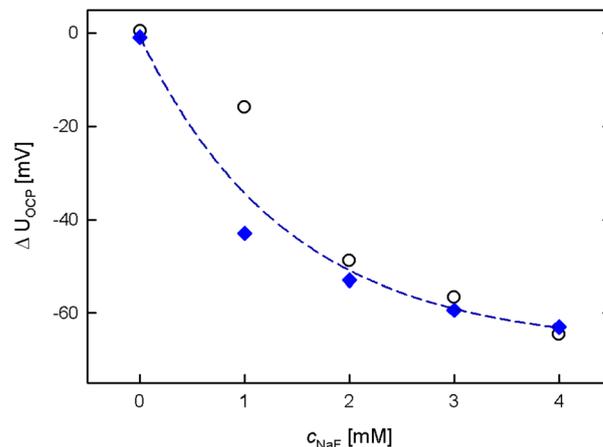

Fig. 5 Mean ΔU_{OCP} upon 1 mM NaF concentration changes of a MPBA modified npAu electrode directly after preparation (black) and after regeneration in 1 M KOH (blue).

detection in water. In Fig. 2 it becomes evident, that the detection concept exhibits clear, immediate responses and a very high sensitivity to very small concentrations of down to 0.2 mM fluoride.

Existing systems such as ion selective electrodes often have long response times[7] or short life spans, as for example systems using ferrocene-terminated surface functionalization.[14,15] Other approaches, which enable detection even in the nano-molar regime, either make use of redox active markers[8,11] or organic buffer solutions,[2,13] which would lead to a pollution of pure water in the in-field use or require lab-based, non-portable measurement setups,[5] which makes an *in situ* use difficult to implement, especially when thinking of mobile environmental applications such as monitoring of water quality. The here presented fluoride indicating electrode for the *in situ* contamination-free use in aqueous solutions stands out by combining very low detection limits with speed and simplicity in its preparation and sensing principle. A comparison of the different fluoride sensing approaches in literature (Table 1) shows that similar advantages can only be found in the work of Liu *et al.*[16] The major difference between the underlying sensing models can be found in the target applications. While the highly sophisticated setup presented by Liu *et al.* is a very fragile system with complicated preparation procedures aiming at high-end applications with highest accuracy demands, the here presented system excels through a simple and fast fabrication which would be easily upscalable as well as easy handling in operation and may therefore be a promising alternative to existing sensing approaches.

The mean ΔU_{OCP} steps presented in Fig. 2c exhibit a clear exponential trend upon addition of different concentrations (0.2 and 1 mM) of NaF and therefore show the accuracy of the created sensing system. The jump heights ΔU_{OCP} (in mV) of both addition rows follow a common exponential decay function:

$$\Delta U_{OCP}(c_{NaF}) = a \times \exp(-b \times c_{NaF}) + c \qquad (1)$$

Table 1 Performance of fluoride detection systems – comparison with literature[a]

Source	Method	LOD [M]	Portable	*In situ*	Non-contaminating	Contaminant
Current article	OCP	2×10^{-4}	Yes	Yes	Yes	
Liu et al.[16]	I–V	10^{-11}	Yes	Yes	Yes	
Yan et al.[8]	DPV	8.3×10^{-10}	Yes	Yes	No	$Fe(CN)_6^{3-}$
Minami et al.[2]	I–V	7×10^{-4}	Yes	Yes	No	MES buffer with NaCl pH 5.5
Ćwik et al.[11]	CV, SWV	10^{-8}	Yes	No	No	NaCl, MES buffer pH 4.0, $Fe(CN)_6^{3-/4-}$
Yue et al.[5]	SERS	10^{-8}	No	No	No	PBS buffer

[a] LOD, limit of detection; *I–V*, current–voltage characteristics; DPV, differential pulse voltammetry; CV, cyclic voltammetry; SWV, square wave voltammetry; SERS, surface-enhanced Raman scattering.

for which coefficients $a = 0.06009$ mV, $b = 1.351$ mM^{-1} and $c = -0.0626$ mV could be fitted for both independent measurements with addition steps of different concentrations c_{NaF} given in mM.

Also the selectivity to F$^-$ over other halide ions has been shown by comparative measurements using Cl$^-$ (Fig. 4). While the response of the nanoporous gold electrode increased drastically towards fluoride upon MPBA modification, the reaction to chlorine was reduced. The remaining signal is most likely caused by chlorine ions still able to access the gold surface. It is well known for gold-SAM systems that there are a lot of defects and the surface coverage is smaller than one monolayer. In this way, some of the Cl$^-$ ions are still able to get to the bare gold surface as illustrated in Fig. 4c leading to the change in surface potential of the electrode as shown in Fig. 4e. In this context, it may be interesting to investigate if a higher surface coverage would lead to a further decrease in the signal due to NaCl addition. Previous studies of our group[18] using different SAM molecules showed, that a longer linking chain length leads to a better surface coverage. As MPBA is a rather small molecule, a study using boronic acid terminated SAMs with different chain lengths would be of interest to further improve the sensitivity and selectivity to F$^-$.

5 Summary and conclusions

Nanoporous gold was successfully modified with 4-mercaptophenylboronic acid, combining the large surface area of the metal with the unique fluoride sensing properties of the boronic acid terminated self-assembled monolayer. In this way a freestanding, easy to handle fluoride sensitive electrode for real-time *in situ* detection of F$^-$ concentrations down to 0.2 mM in water was obtained. Exposing the sample to a step-wise increasing fluoride concentration leads to immediate and well-defined changes of the surface potential, which results from the change in hybridization and therefore charge distribution of the functional boronic acid group of the SAM when it binds fluoride ions. Those potential changes were well reproducible, even after the regeneration of the modified electrode in alkaline conditions for several times. In-depth analysis using electrochemical impedance spectroscopy measurements in 50 mM KNO$_3$ were performed to monitor the fluoride binding process and showed an ongoing reaction at the electrode's

surface directly after fluoride addition. After reaching an equilibrium, the electrode exhibited an increased capacitance, which is assigned to the accumulation of fluoride at the SAM. The surface potential of the modified npAu sample was also measured upon the addition of chlorine. The strong reaction of the pristine npAu sample with Cl$^-$ was drastically decreased by the modification with the SAM, leaving only a small rest signal most probably due to some ions still reaching the gold surface through imperfections in the SAM. This signal reduction clearly shows the selectivity of the chosen surface modification towards fluoride.

The created electrode has many advantages for a fast and simple detection of F$^-$ and therefore potential for several portable applications, such as (waste-)water analysis, in the future. In this context, it may be interesting to investigate the influence of different linking chain lengths of boronic acid terminated SAMs on the surface coverage and, if possible, further improve the selectivity towards fluoride over other halogenic species. Moreover, employing the high specificity of a functional surface group to a certain chemical species as a sensor principle in combination with the high active surface area of npAu samples has large application potential, not only in halide detection, but in various areas of high scientific and societal interest. As a specific example, the concept would be ideal to exploit the specific binding of hormones to their receptor units for highly efficient biosensors.

Conflicts of interest

There are no conflicts to declare.

Acknowledgements

Notes and references

1 K. Gobi and T. Ohsaka, *J. Electroanal. Chem.*, 2000, **485**, 61–70.
2 T. Minami, T. Minamiki and S. Tokito, *Chem. Commun.*, 2015, **51**, 9491–9494.

3 X.-F. Yang, S.-J. Ye, Q. Bai and X.-Q. Wang, *J. Fluoresc.*, 2007, **17**, 81–87.

4 P. Gao, X. Tian, C. Yang, Z. Zhou, Y. Li, Y. Wang and S. Komarneni, *Environ. Sci.: Nano*, 2016, **3**, 1416–1424.

5 X. Yue, Y. Su, X. Wang, L. Li, W. Ji and Y. Ozaki, *ACS Sens.*, 2019, **4**, 2336–2342.

6 Y. Zhou, J. F. Zhang and J. Yoon, *Chem. Rev.*, 2014, **114**, 5511–5571.

7 C. Maccà, *Anal. Chim. Acta*, 2004, **512**, 183–190.

8 F. Yan, X. Ma, Q. Jin, Y. Tong, H. Tang, X. Lin and J. Liu, *Microchim. Acta*, 2020, **187**, 1436–5073.

9 X. Deng, X. Lin, H. Zhou, J. Liu and H. Tang, *Nanomaterials*, 2023, **13**, 239.

10 J. Gong, H. Tang, M. Wang, X. Lin, K. Wang and J. Liu, *Mater. Des.*, 2022, **215**, 110506.

11 P. Ćwik, U. E. Wawrzyniak, M. Jańczyk and W. Wróblewski, *Talanta*, 2014, **119**, 5–10.

12 A. Maikap, K. Mukherjee, N. Mandal, B. Mondal and A. Meikap, *Electrochim. Acta*, 2018, **264**, 150–156.

13 M. Nicolas, B. Fabre and J. Simonet, *Electrochim. Acta*, 2001, **46**, 1179–1190.

14 L. L. Norman and A. Badia, *J. Phys. Chem. C*, 2011, **115**, 1985–1995.

15 G. Valincius, G. Niaura, B. Kazakevičienė, Z. Talaikytė, M. Kažemėkaitė, E. Butkus and V. Razumas, *Langmuir*, 2004, **20**, 6631–6638.

16 Q. Liu, K. Xiao, L. Wen, Y. Dong, G. Xie, Z. Zhang, Z. Bo and L. Jiang, *ACS Nano*, 2014, **8**, 12292–12299.

17 A. Aydogan, A. Koca, M. K. Şener and J. L. Sessler, *Org. Lett.*, 2014, **16**, 3764–3767.

18 E. Hengge, M. Hirber, P. Brunner, E.-M. Steyskal, B. Nidetzky and R. Würschum, *Phys. Chem. Chem. Phys.*, 2021, **23**, 14457–14464.

19 E. Hengge, E.-M. Steyskal, R. Bachler, A. Dennig, B. Nidetzky and R. Würschum, *Beilstein J. Nanotechnol.*, 2019, **10**, 2275–2279.

20 E.-M. Steyskal, M. Seidl, M. Graf and R. Würschum, *Phys. Chem. Chem. Phys.*, 2017, **19**, 29880–29885.

21 O. Polat and E. Seker, *J. Phys.Chem. C*, 2015, **119**, 24812–24818.

22 A. D. Marderosian and C. Murphy, *15th International Reliability Physics Symposium*, 1977, pp. 92–100.

23 J. Lipkowski, Z. Shi, A. Chen, B. Pettinger and C. Bilger, *Electrochim. Acta*, 1998, **43**, 2875–2888.

24 N. Mameka, L. Lührs, S. Heissler, H. Gliemann and C. Wöll, *ACS Appl. Nano Mater.*, 2018, **1**, 6613–6621.

25 E. Galbraith and T. D. James, *Chem. Soc. Rev.*, 2010, **39**, 3831–3842.

26 X. Chen, G. Zhou, S. Mao and J. Chen, *Environ. Sci.: Nano*, 2018, **5**, 837–862.

27 C. Lakshmanan, R. Viswanath, S. Polaki and R. Rajaraman, *AIP Conference Proceedings*, Melville, NY, 2015, p. 140033.

28 M. E. Orazem and B. Tribollet, *Electrochemical Impedance Spectroscopy*, John Wiley & Sons, Ltd, 2017, pp. 493–526.

29 T. Pajkossy, T. Wandlowski and D. M. Kolb, *J. Electroanal. Chem.*, 1996, **414**, 209–220.

30 T. M. Nahir and E. F. Bowden, *Langmuir*, 2002, **18**, 5283–5286.

31 A. Borovik, V. Karanikola and I. Zucker, *Environ. Sci.: Nano*, 2020, **7**, 3641–3654.